International Journal for Housing Science and Its Applications

Publish September 8, 2025. Volume 47, Issue 1 Pages 44-59

https://doi.org/10.70517/ijhsa47104

Research on a dual-drone cooperative formation flight algorithm based on distributed control

Yarong Hu[1], Buyong Ren[1], Sifan Chen[1], Junyun Shen[1] and Yonglong Ma[1,*]

[1] Linxia Power Supply Company, State Grid Corporation of China, Linxia, Gansu, 731800, China

Corresponding authors: (e-mail: xmzy_fzu@163.com).

Abstract With the advancement of science and technology, unmanned aerial vehicles (UAVs) are playing an increasingly important role across various fields, making multi-UAV formations a cutting-edge research area. This study establishes a UAV communication topology model based on graph theory and proposes a UAV motion model based on spatial position deviations. A distributed structure is then introduced to design a UAV control system model and establish a UAV formation coordination mechanism. Based on this, a coordination formation controller using a consensus algorithm, a task allocation strategy using the Hungarian algorithm, and an obstacle avoidance strategy are designed. Simulation experiments were conducted with a five-drone formation executing reconnaissance tasks and a triangular formation. The simulation results indicate that the designed control algorithm can maintain the formation of the drone formation, the proposed collaborative control strategy can achieve precise formation maintenance, and it can quickly and accurately track the predefined flight path. During formation flight, collisions between adjacent drones can be avoided, and the formation has excellent reconstruction capabilities, achieving stable and accurate collaborative formation.

Index Terms distributed structure, cooperative control, Hungarian algorithm, formation maintenance, drone formation

I. Introduction

Today, fifth-generation mobile communication technology (5G) has permeated virtually every aspect of people's lives, and the Internet of Things (IoT) technology has also seen rapid development. Concepts such as "unmanned smart agriculture," "smart manufacturing," and "unmanned system collaboration" have been widely proposed. Unmanned systems, leveraging the high bandwidth and low latency characteristics of 5G, are increasingly gaining attention. Drones, as a representative example of unmanned systems, play an undeniably crucial role [1], [2]. For instance, drone technology can be deployed in military applications such as intelligence gathering, precision strikes, and terrain reconnaissance, as well as in civilian sectors for tasks like pesticide spraying, fire detection, photography, and performances [3]-[6].

However, when a single drone performs a mission, its physical parameters limit its performance, affecting mission success rates. Additionally, if a single drone is destroyed or malfunctions, it may disrupt the entire operational plan [7]-[9]. To enhance mission completion rates and efficiency, achieving multi-drone cooperative flight is a current research focus. On one hand, establishing a reasonable multi-drone flight formation is simpler than increasing the number of drones operated individually [10], [11]. On the other hand, multi-UAV coordination can expand the types of tasks that can be completed and improve task completion quality and efficiency [12], [13]. As UAVs are applied in more scenarios, multi-UAV coordination formations will become an important application method for UAVs, profoundly impacting people's lives [14].

UAV swarm technology is the key to achieving multi-UAV formation flight while ensuring that collisions between nodes are avoided [15]. Under the support of swarm technology, UAVs utilize high-reliability information and communication technology to achieve comprehensive information interconnection among single UAVs and the swarm, single UAVs and ground stations, swarm and ground stations, and swarm and swarm [16]-[18]. However, current multi-UAV swarm technology still faces numerous challenges, such as intelligent self-organizing network communication issues related to swarm network interference resistance and communication latency, as well as limited physical applications of UAV swarm platforms and a reliance on simulation verification for algorithm validation [19]-[22]. Additionally, traditional UAV swarm communication management technologies have significant security issues, such as single points of failure caused by centralized management and the absence of reliable identity verification mechanisms for data interaction [23]-[25]. Based on this, cluster control algorithms can be optimized by focusing on the interaction strategies and control methods of drone clusters, aiming to enhance the feasibility of drone cluster applications.

As the core control logic for formation flight missions, the performance of the algorithms carried by the drone cluster

platform is a decisive factor in the success of flight missions. Currently, the academic community has achieved significant results in the field of swarm intelligence, and domestic and international research teams are gradually introducing swarm intelligence algorithms into unmanned systems and exploring their application effects. Gao, S., and Zeng, C., et al., improved the classic ant colony optimization (ACO) algorithm using cubic mapping, optimizing the initial distribution and pheromone concentration update mechanism to effectively address issues such as slow convergence speed and tendency to get stuck in local optima when applied to dense drone formation control [26]. Yang, Z, and others explored a drone formation reconstruction strategy based on an improved artificial bee colony (ABC) algorithm. They first constructed a formalized model of the formation reconstruction problem with time minimization as the objective, while reducing the influence of drone formation control parameters. The results showed that the improved ABC algorithm exhibits excellent formation reconstruction performance [27]. Chen, J et al. introduced pheromone factors into the traditional gray wolf optimization algorithm (GWO). The proposed improved GWO algorithm effectively addressed the instability issues in swarm cooperative trajectory optimization under dynamic environments, facilitating low-cost swarm cooperative trajectory optimization [28]. Gao, C et al. proposed an adaptive hybrid particle swarm and differential evolution algorithm to reduce the computational cost of formation reconstruction. By using the shortest movement distance as the flight control input, they achieved good cooperative control of the drone formation [29]. Hoang, V. T., et al. utilized an angle-coded particle swarm optimization algorithm to optimize the flight paths of a drone swarm. By collecting the angular velocity and position of particles, the position of the drones was determined, achieving good cooperative formation control effects [30]. Swarm intelligence algorithms applied to drone formation control have the characteristics of low cost and high autonomy, enabling dynamic adaptive adjustments in complex environments.

Additionally, well-known and relatively simple formation control algorithms include the artificial potential field algorithm and the leader-follower consistency algorithm. Zhang, J., et al. addressed the obstacle avoidance problem for multi-UAV formations by proposing an improved artificial potential field algorithm to calculate the gravitational and repulsive forces between each UAV, thereby planning collision-free flight paths that maintain formation for the UAV formation [31]. Wang, N et al. combined the artificial potential field method and consistency theory to design a multi-UAV cooperative formation obstacle avoidance control protocol. The proposed algorithm not only enhances the obstacle avoidance capability of the UAV formation and reduces the collision probability but also achieves consistency in relative distance, relative altitude, and speed [32]. Wu, E et al. introduced a virtual core into the drone formation and utilized the gravitational and repulsive forces of the artificial potential field algorithm to control the flight trajectories of drones, thereby improving the collaborative efficiency and obstacle avoidance capabilities of the swarm during flight [33]. Guerrero-Castellanos, J. F et al. investigated communication event-triggered drone formation control strategies, combining internal and external control methods of the leader-follower algorithm to achieve consistency in the positions of the drone swarm [34]. DURDU, A., and KAYABAŞI, A. examined drone swarm control strategies in scenarios involving drone crashes and communication interruptions. The proposed virtual leader tracking algorithm can innovate new swarm shapes in such scenarios, endowing the drone swarm structure with higher robustness and flexibility [35]. Yang, K., et al. pointed out that backstepping adaptive control based on predefined performance can ensure that UAVs quickly track their respective reference trajectories while effectively avoiding external disturbances and formation collisions during trajectory tracking, thereby maximizing the realization of the desired formation configuration [36]. The aforementioned studies have made various improvements to artificial potential field algorithms and leader-follower consistency algorithms, resulting in formation control algorithms with high practicality and reliability.
However, the aforementioned swarm UAV control schemes are often affected by issues such as high development difficulty, poor damage resistance, and poor stability. This is because centralized control algorithms heavily rely on the computational performance of onboard computers, which have limited performance in large-scale formation problems. Therefore, distributed formations will become the mainstream for future unmanned systems.

Using graph theory to describe the communication topology structure of UAV formations, this study proposes a UAV motion model based on relative position, simplifying the UAV dynamics model. Additionally, addressing the three-dimensional formation control problem in multi-UAV systems, a distributed consistent UAV formation cooperative control method is proposed. The Hungarian algorithm is employed to minimize distance costs during formation transitions, and a simple yet effective obstacle avoidance algorithm is introduced. Finally, position, velocity, and heading are introduced as cooperative variables, and the simulation results are analyzed. During formation maintenance simulations, a triangular formation is designed, and formation transformation experiments are conducted during obstacle avoidance.

II. Modeling of unmanned aerial vehicle formation systems

II. A. Defining Communication Topology Diagrams

II. A. 1) Fundamentals of Graph Theory

Graph theory is a very important part of applied mathematics and has a wide range of applications in complex networks, where it is used to study specific relationships between certain things. Graph theory also has a large number of applications in the study of multi-agent consensus control [37]. The advantage of graph theory lies in the fact that it has three main matrix forms

that can clearly describe the connection between multi-agents and facilitate system stability analysis. The main matrix forms in graph theory are as follows:

(1) Adjacency matrix A_n

The adjacency matrix $A_n = \left[a_{ij} \right] \in R^{n \times n}$ represented by directed graph (V_n, E_n) is defined as follows: when $(j,i) \in E_n$ exists, i.e., node i can receive information from node j, then $a_{ij} > 0$; when $(j,i) \notin E_n$ exists, then $a_{ij} = 0$. Since self-edges are ignored, $a_{ii} = 0$. Similarly, in an undirected graph, for all $i \neq j$, $a_{ij} = a_{ji}$. The weight of an edge in the adjacency matrix has no specific practical definition, so when $(j,i) \in E_n$ exists, the value of a_{ij} can be defined as l.

(2) In-degree matrix D In a directed graph with n independent nodes, the in-degree value of the i th node is $d_{ii} = \sum_{j=1, j \neq i}^{n} a_{ij}$. The in-degree matrix can be represented by $D = diag\{d_{ii}\}$.

(3) Laplacian matrix L_n

Define the matrix $L_n = \left[l_{ij} \right] \in R^{n \times n}$ as:

$$l_{ij} = \begin{cases} -a_{ij} & i \neq j \\ \sum_{j=1, j \neq i}^{n} a_{ij} & i = j \end{cases} \tag{1}$$

Here, $L_n = \left[l_{ij} \right] \in R^{n \times n}$ can also be defined equivalently as $L_n = D - A_n$, where $D = \left[d_{ij} \right] \in R^{n \times n}$ is an "in-degree matrix." For any $(j,i) \notin E_n$, there exists $l_{ij} = -a_{ij} = 0$, and matrix L_n satisfies:

$$l_{ij} \leq 0, i \neq j, \text{ and } \sum_{j=1}^{n} l_{ij} = 0, i = 1, 2, ...n \tag{2}$$

The asymmetric L_n is referred to as the "directed Laplacian matrix" or "asymmetric Laplacian matrix" of a directed graph. For an undirected graph, L_n is symmetric, and in this case, L_n is referred to as the "Laplacian matrix" of the undirected graph. The Laplacian matrices of directed and undirected graphs share a common property: they both have a simple zero eigenvalue, corresponding to an $n \times 1$ eigenvector 1_n whose elements are all 1.

II. A. 2) Unmanned Aerial Vehicle Communication Topology

This paper establishes the communication range of regional formation drones based on graph theory, as shown in Figure 1, which describes the information interaction between drones within the regional formation. Define an undirected graph G and represent it using (V, E), where:

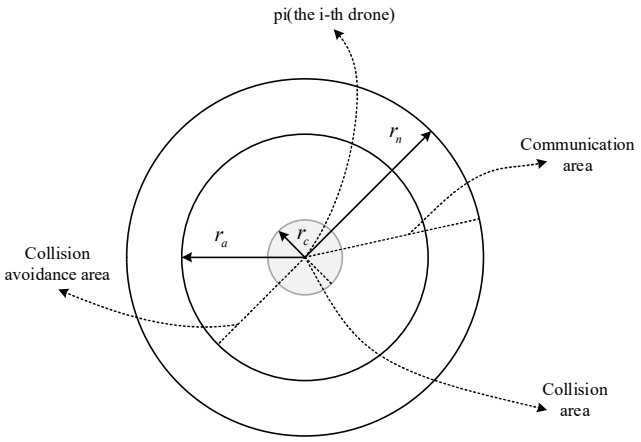

Figure 1: A cross section of the restricted area of the drone i

$V = \{i = 1, 2, ..., n\}$ is a set of n non-empty nodes, representing the information exchange relationships among n drones within an unmanned aerial vehicle (UAV) formation in an undirected graph. Define the undirected graph G and represent it

using (V,E) pairs of undirected graphs, where the set of communication network vectors, $E=\{k_{ij}:i=1,2,...,n:j\in N_i\}$, is referred to as the set of node pairs known as "edges," representing the communication connection relationships between drones in the formation. The set of neighbors of the i th drone, N_i, is defined as: $N_i \square \{j\in V\}$.

To prevent collisions between UAVs in a regional formation, this paper defines the collision avoidance region D_i, communication region Ω_i, and collision region C_i for UAVs in a coordinated formation. The mathematical models for these three regions are expressed as follows:

$$\begin{aligned} D_i &\square \{j\in V: r_c < d_{ij} \le r_a, i\ne j\} \\ \Omega_i &\square \{j\in V: r_c < d_{ij} \le r_n, i\ne j\} \\ C_i &\square \{j\in V: d_{ij} \le r_c, i\ne j\} \end{aligned} \tag{3}$$

where: $d_{ij} = \| p_i - p_j \|_2$.

In Figure 1, $p_i(t)\in R^3$ and $p_j(t)\in R^3$ represent UAV_i and UAV_j respectively, r_c is the radius of the drone body, r_a is the radius of the drone collision avoidance region, and N_i is the neighbor set of the i th drone, and r_n is the maximum collision detection region radius constant, satisfying $r_n > r_a$.

II. B. Formation Description

II. B. 1) Commonly Used Coordinate Systems

When considering the coordinated formation flight of drones in three-dimensional space, each drone will have six degrees of freedom. To clearly and accurately describe the flight status of the drone formation, selecting an appropriate reference coordinate system for the drone formation becomes particularly important. The two commonly used reference coordinate systems are as follows.

(1) Ground Inertial Coordinate System

The basic principle of the ground inertial coordinate system is to select any point on the Earth's surface as the origin O of the three-dimensional coordinate system. The OX coordinate axis is chosen in any direction from the origin O on the horizontal plane of the Earth's surface, and the OZ coordinate axis is perpendicular to the origin O and points upward. The OY coordinate axis is perpendicular to the OX coordinate axis on the Earth's surface, and the three coordinate axes in three-dimensional space satisfy the right-hand rule. The ground inertial coordinate system provides a good reference benchmark for describing the flight position information of unmanned aerial vehicle formations.

(2) Unmanned Aerial Vehicle Heading Coordinate System

Unlike the ground inertial coordinate system, the unmanned aerial vehicle heading coordinate system is based on the real-time flight position of the unmanned aerial vehicle in the formation. The basic principle of this coordinate system is to define the center of mass of the drones in the formation as the origin O' of the three-dimensional coordinate system. The direction defined as the same as the flight speed direction of the drones is defined as the OX" coordinate axis, and the direction that is in the same horizontal plane as the OX' coordinate axis in three-dimensional space and perpendicular to the OX' coordinate axis is defined as the OY' The OZ coordinate axis in three-dimensional space is perpendicular to the X'OY' plane formed by the OX' and OY' coordinate axes, and the three coordinate axes in three-dimensional space also satisfy the right-hand rule.

II. B. 2) Formation Shape Description

Define the inequality of the target function for the drone formation as follows:

$$f_G(\Delta p_i) = \left[f_{G1}(\Delta p_{i01}), f_{G2}(\Delta p_{i02}), ..., f_{GM}(\Delta p_{i0M})\right]^T \le 0 \tag{4}$$

In formula (4), $\Delta p_{i0l} = p_i - p_{0l}$, where $p_{0l}(t)$ is the reference point position within the i th expected region, and $l=1,2,\ldots,M$; M denotes the total number of formation constraint conditions for the unmanned aerial vehicle (UAV) cooperative formation, and $f_{Gl}(\Delta p_{i0l})$ is a continuous scalar function with continuous partial derivatives. When $\| \Delta p_{i0l} \| \to \infty$, then $| f_{Gl}(\Delta p_{i0l}) | \to \infty$. $f_G(\Delta p_{i0l})$ is bounded, thereby ensuring that $\frac{\partial f_{Gl}(\Delta p_{i0l})}{\partial \Delta p_{i0l}}, \frac{\partial^2 f_{Gl}(\Delta p_{i0l})}{\partial \Delta p_{i0l}^2}$ are bounded. Each reference point in a single independent region is chosen as a constant offset relative to the others, so that $\dot{p}_{0l} = \dot{p}_0$, where $\dot{p}_0$ is the velocity of the desired formation.

II. C. Mathematical Model of Unmanned Aerial Vehicle Motion

This study primarily focuses on control algorithm research for drone formation flight under ideal conditions, where drones share identical airframes and rotors, and communication latency issues in drone systems are assumed to be absent. These factors would otherwise complicate the research. To simplify the analysis, the study assumes that none of these potential influencing factors exist. Depending on the focus of the research problem, to simplify the complexity of the controlled object, the drone formation control is treated as control between multiple nodes in three-dimensional space during the generation and maintenance of the drone formation. Therefore, after simplifying the mathematical model of a single drone, the following can be obtained:

This chapter considers a drone formation flight control system consisting of n UAVs, where the mathematical model of the i th drone can be expressed as:

$$\begin{cases} \dot{p}_{1,i}(t) = v_{1,i}(t) \\ \dot{v}_{1,i}(t) = u_{1,i}(t) \\ y_{1,i}(t) = p_{1,i}(t) \end{cases} \tag{5}$$

where: $i = 1,2,3,...,n$, $p_{1,i}(t) \in R^3$ and $v_{1,i}(t) \in R^3$ are the position and velocity values of the i th drone, and $u_{1,i}(t) \in R^3$ is the control input.

III. Distributed UAV cooperative formation design

III. A. Mechanistic modeling

III. A. 1) Control System Model

The cooperative control of unmanned aerial vehicle (UAV) formations consists of two components: the cooperative flight control system and the cooperative trajectory control system. The cooperative flight control system serves as the inner loop, controlling the flight attitude; the cooperative trajectory control system acts as the outer loop, controlling the flight trajectory, with its output serving as the input for the inner loop. The cooperative trajectory control system calculates the corresponding attitude information, such as pitch angle, yaw angle, and speed, based on the desired movement position, and transmits this information to the cooperative flight control system. Upon receiving the commands, the flight control system calculates the rotor thrust based on the new attitude information and sends motor commands to control the movement. If no predefined flight path is set, the formation can fly freely, and the trajectory control task becomes simpler, requiring only collision avoidance during flight. In this paper's drone formation cooperative control system, a feedback control law based on a consistency algorithm is designed to accomplish formation and attitude coordination tasks.

III. A. 2) Distributed Structure

Compared with traditional centralized cooperative formation control theory, cooperative formation control methods based on distributed structures offer advantages such as flexible communication control frameworks, unlimited individual numbers, low computational requirements, and ease of engineering implementation. Communication between UAVs is bidirectional, and bidirectional communication facilitates cooperative flight of UAV formations to complete various tasks. At the same time, when the number of UAVs in the formation increases to three or more, stability and reliability can be improved.

(1) UAV Commander

The UAV commander plays a command and control role within the UAV formation, guiding the entire team to fly along a predefined flight path. It maintains real-time communication with the ground control center and other UAVs. The mission process is pre-installed on each UAV and can be activated by the ground control station in the event of the leader's failure.

(2) Drone Follower

Drone followers follow their leader. They maintain contact with the ground control center and continuously receive commands from the drone commander. Communication is also possible between every two drone followers. This paper combines the “veteran rule” with the classic “leader-follower” communication mechanism, designing various experience values based on the distance between local leaders and local followers, and can then easily obtain the expected Laplace matrix L.

III. A. 3) Coordination Mechanism

Based on the distributed structure established above, combined with intelligent swarm theory and specific practical circumstances, the following collaborative mechanisms are proposed for drone formation processes:

(1) Consistency

Given a formation structure, the drone leader flies toward the specified position and distributes the leader's relevant pose

information to the corresponding drone followers, enabling them to achieve consistency in position and velocity.

(2) Task allocation

The drone followers receive information from the drone leader, and the primary task of each drone follower is to fly toward the desired position.

(3) Collision avoidance

A safety distance $D(0 < D < R)$ is pre-set. If the minimum distance between each pair of UAVs is reduced to D, corresponding measures will be taken to avoid collisions.

The above three steps of the coordination mechanism are the tasks that each drone needs to follow and complete. They will be elaborated in detail in the next chapter on coordinated formation design.

III. B. Dual drone cooperative formation flight

III. B. 1) Consistency-based cooperative formation controller

Considering a set of N UAVs, each UAV can be modeled as an integrator model based on its dynamic model, which can be described as:

$$\dot{\xi}_i = \mu_i, \dot{\mu} = a_i, i = 1,2,\cdots,N \tag{6}$$

Here, a_i is the acceleration of UAV_i, and ξ_i and μ_i are the position and velocity states of UAV_i, respectively. All UAVs move in an m-dimensional space, where $m = 3$ in this simulation. The target state is for all UAVs to reach a given formation pattern. The formation controller is as follows:

$$c_i = -\sum_{j=1}^{N} \omega_{ij} \{[(\xi_i - \delta_i) - (\xi_j - \delta_j)] + \gamma(\mu_i - \mu_j)\} \tag{7}$$

$$W = [\omega_{ij}] \in R^{N \times N} \tag{8}$$

ω_{ij} is an element of the adjacency matrix W. When and only when $\omega_{ij} > 0$, it indicates that UAV_j communicates with UAV_i communicate. δ_i is the formation offset of drone i, determined by the final desired formation configuration and its desired position. γ_i is an adjustable parameter related to the stability and convergence of the system.

When $\| (\xi_i - \delta_i) - (\xi_j - \delta_j) \| \to 0$ and $\| \mu_i - \mu_j \| \to 0$, the system is considered to have achieved consistency.

Since system consistency is equivalent to formation stability, the system described in this paper can achieve formation stability.

For n unmanned aerial vehicles, define their communication topology structure as G_n, and let L be the corresponding Laplacian matrix of G_n. Let $L = [l_{ij}] \in R^{N \times N}$, and its elements are defined as:

$$l_{ij} = \begin{cases} \sum_{j=1, j \neq i}^{N} \omega_{ij}, i = j \\ -\omega_{ij}, i \neq j \end{cases} \tag{9}$$

Let $c = [c_1, c_2, \cdots, c_N]^T$, $\xi = [\xi_1, \xi_2, \cdots, \xi_N]^T$, $\delta = [\delta_1, \delta_2, \cdots, \delta_N]^T$, $\mu = [\mu_1, \mu_2, \cdots, \mu_N]^T$ then system (9) can be written as:

$$c = (-L \otimes I_m)(\xi - \delta) - \gamma(L \otimes I_m)\mu \tag{10}$$

Here $I_m = [1,1,\cdots,1]^T \in R^m$, in this simulation $m = 3$.

Considering the setting of parameter γ, the system reaches stability when and only when the following conditions are met:

$$\gamma > \max_{i=1,2,\cdots,N} \sqrt{\frac{2}{|\lambda_i| \cos[\tan^{-1} \frac{\mathrm{Im}(\lambda_i)}{\mathrm{Re}(\lambda_i)}]}} \tag{11}$$

λ_i is the i th eigenvalue of $-L$, and $\mathrm{Re}(\lambda_i)$ and $\mathrm{Im}(\lambda_i)$ are the real and imaginary parts of λ_i, respectively. It is clear that the parameters originally satisfying condition (11) become fragile after changing the matrix L, which may significantly reduce the scalability of the simulation platform. Therefore, for any number of drones, there is a strong need for universal communication topology rules and parameters γ.

III. B. 2) Task allocation

To reduce the difficulty of distributed task allocation and take into account the characteristics of the simulation platform, a variant of the Kuhn-Munkres algorithm is used for task allocation.

Consider the current vertex positions of n drones and their transformed vertex positions as two sets of vertices. There are no edges between any two vertices within a set, and only edges exist between the two sets. Let this be the bipartite graph A. The objective of this section is to achieve a perfect matching of the bipartite graph, i.e., there are $n!$ bijective matching combinations between the two sets. The value of each element a_{ij} in A represents the distance d_{ij} between the previous formation offset and the current formation offset, i.e., the weight or cost of this edge. The algorithm flow is as follows:

(1) Initialize the weights of each feasible route for the drones.

(2) Use the Hungarian maximum matching algorithm to determine if there is an augmenting path that meets the conditions.

(3) If an augmenting path is found, update the values of the current feasible routes.

(4) Repeat steps (2) and (3) until the optimal matching is found.

The allocation obtained by this algorithm is the optimal grouping with the minimum total cost.

III. B. 3) Obstacle avoidance strategy

Figure 2 shows the obstacle avoidance strategy. Assuming that the information sensing range of the UAV is a spherical body, R is the maximum communication radius of the UAV, d is the maximum safe obstacle avoidance radius of the UAV, r is the distance vector between the two UAVs, pointing to the obstacle UAV within the safe range, a is the obstacle avoidance vector of UAV1, and a' is the obstacle avoidance vector of UAV2. a and a' are opposite in direction and perpendicular to r.

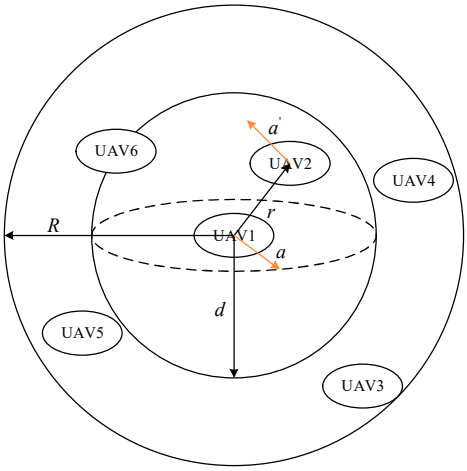

Figure 2: Avoidance strategies

IV. Simulation experiments and analysis

IV. A. Simulation parameter settings

At the initial moment, *UAV* s in different positions receive mission instructions, take off separately, and form a close-range "V" formation to fly to the target area. Upon reaching the target area, they receive ground instructions to spread out, forming a long-range "V"-shaped formation to expand the search range. After circling the target area twice and acquiring reconnaissance imagery, they revert to a close-range "V"-shaped formation and fly to the next target area. The initial states of each *UAV* are shown in Table 1, and the formation structure is shown in Table 2.

Table 1: Initial state of each UAV formation

UAV	Position /m	Velocity /m/s	Path angle /rad
Virtual long machine	(50,50,0)	0	π /10
UAV 1	(11,0,0)	0	π /5
UAV 2	(25,-35,0)	0	π /7
UAV 3	(50,0,0)	0	π /2
UAV 4	(25,-15,0)	0	π /4
UAV 5	(40,10,0)	0	π /3

Table 2: Define formation for different mission phases

UAV	The patrol formation /m	Formation of the investigation /m
UAV 1	(11,0,0)	(11,0,0)
UAV 2	(25,11,0)	(25,22,0)
UAV 3	(25,-11,0)	(25,-11,0)
UAV 4	(35,25,0)	(35,50,0)
UAV 5	(35,-25,0)	(35,-50,0)

Based on the requirements of the reconnaissance mission, formation adjustment commands are sent from the ground, and these commands can be considered as external disturbances to the formation flight process. Through formation change simulation, the response of the formation maintenance control algorithm to external disturbances is obtained. The virtual lead aircraft reference trajectory command is:

$$a_L = \begin{cases} 10m/s^2, t \in [0,3)s \\ 0, others \end{cases} \tag{12}$$

$$\omega_{xL} = \begin{cases} \pi/10 rad/s, t \in [21,25) \cup [45,90)s \\ 0, others \end{cases} \tag{13}$$

$$\omega_{yL} = \begin{cases} \pi/12 rad/s, t \in [0,4)s \\ 0, others \\ -\pi/12 rad/s, t \in [10,14)s \end{cases} \tag{14}$$

Other parameters: Virtual long-range state estimation algorithm convergence coefficient $\lambda = 0.5$, UAV autopilot model parameters $\tau_V = 1, \tau_X = 0.33, \tau_{h_a} = 1, \tau_{h_b} = 1$, controller parameters as shown in Table 3.

Table 3: Prepare channel controller parameters

Channel	Position error	Mobility error	Scale	Integration	Differentiation
Velocity	11	2	9.76	17.31	2.03
Azimuth	5	2	0.58	0.06	0.11
Altitude	2	-	6.46	2.74	1.79

IV. B. Formation flight simulation with no obstacles

The reference positions of each drone in the triangular formation are designed as shown in the figure. The initial position of the lead drone is set to (11, 16, 6) km, while the initial positions of the two wing drones are (6, 30, 5) km and (6, 25, 5) km, respectively. Figure 3 is a simulation diagram of the triangular formation control of the drone formation. The simulation diagram shows the process of the drone formation advancing from the initial position, forming a triangular formation, maintaining the triangular formation while flying forward, and finally heading toward the target position. The final spacing distances in the X, Y, and Z directions are 210, 210, and 110 m, respectively.

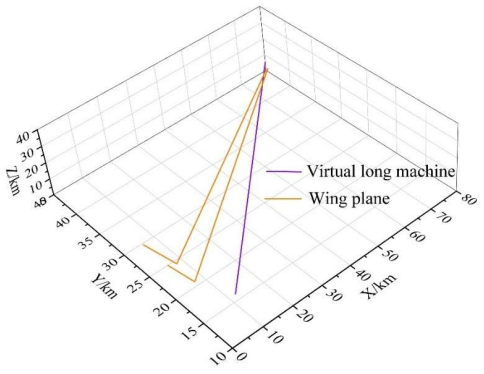

Figure 3: Keep the triangle formation when accessible

When the formation maintains flight, the lateral, longitudinal, and altitude distances between the drones all meet the required formation spacing requirements, as shown in Figures 4-6. Taking the formation spacing between the lead aircraft and wingman 2 as an example, it can be seen from the simulation diagram shown that the drone formation can maintain a good triangular formation during movement.

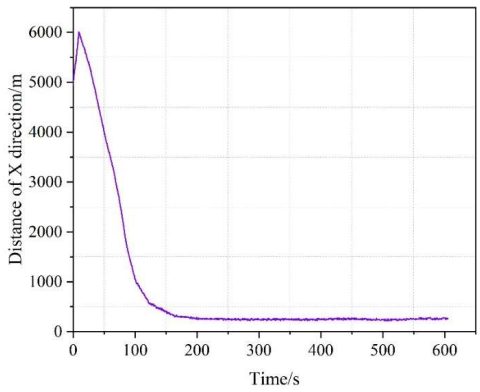

Figure 4: The distance in the x direction when accessibility is enabled

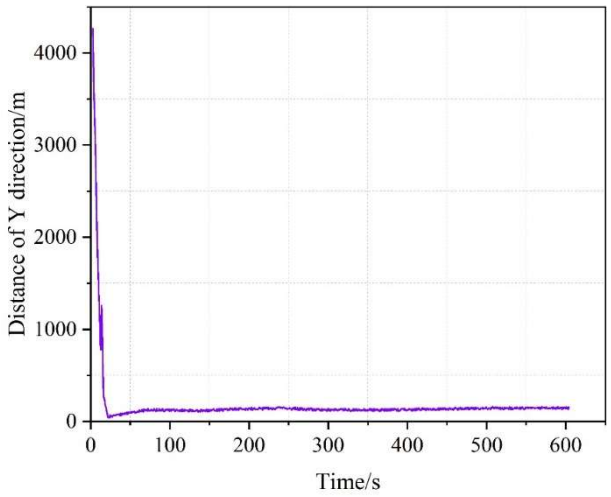

Figure 5: The distance in the y direction when accessibility is enabled

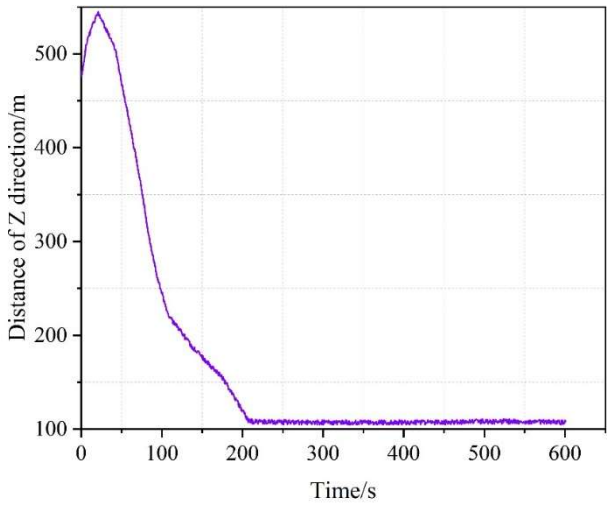

Figure 6: The distance in the z direction when accessibility is enabled

This paper introduces a cooperative mechanism into formation maintenance behavior, enabling the formation process to be

more rapid. The change in speed of the drone formation from formation to maintenance is shown in Figure 7. The initial speed of the drones is 100 m/s, with a maximum speed of 183 m/s. Once the formation is stable, the speed is maintained at 157 m/s.

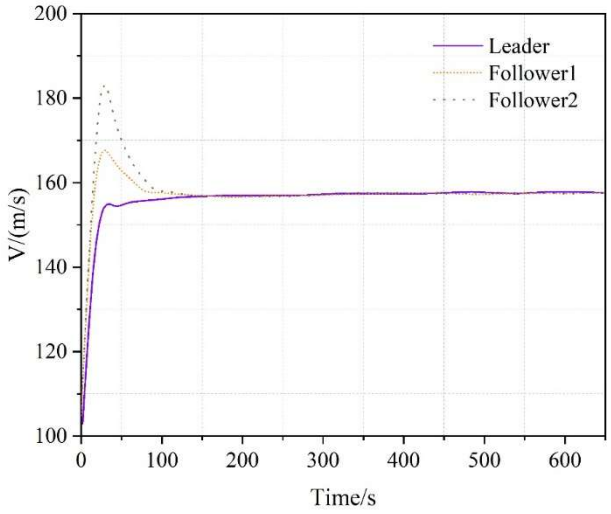

Figure 7: The formation maintains a speed change

IV. C. Simulation and verification of collision avoidance and formation changes for unmanned aerial vehicle fleets

IV. C. 1) UAV Formation Maintenance Simulation and Verification

Based on the above content, a Simulink model was constructed. Figure 8 shows the simulation results of five UAVs performing reconnaissance tasks in a "V" formation. It can be seen that the UAVs, which initially started from different positions, quickly converged to the desired formation and flew along the reference trajectory. The coordinated turning effect was ideal, and they were able to respond to formation adjustment commands to perform reconnaissance tasks. Figure 9 shows the estimated error curves between the virtual lead aircraft positions and actual positions of each UAV, which gradually stabilize near zero, verifying that the cooperative formation controller can serve as a guidance system for formation drones.

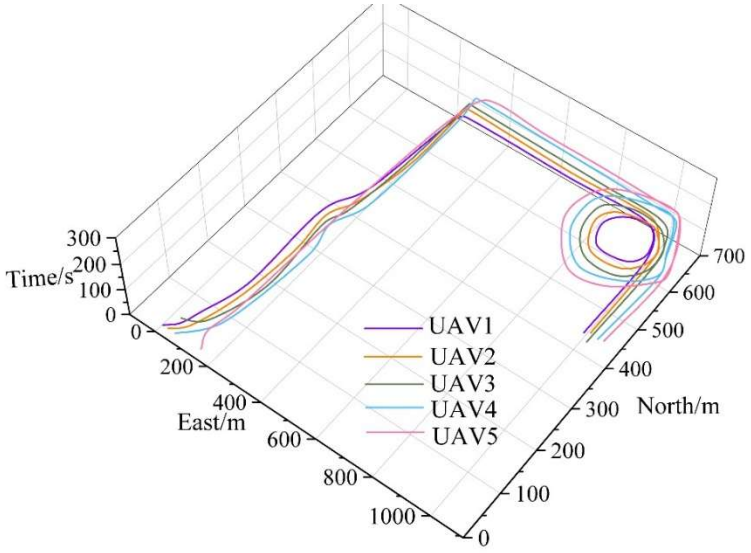

Figure 8: "V" -shaped formation for reconnaissance mission simulation

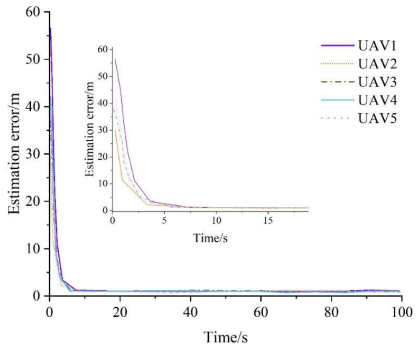

Figure 9: Error of each UAV's virtual long machine position estimation

Figures 10 and 11 show the longitudinal and lateral formation error curves for each UAV during formation flight, respectively. The UAVs take off from random initial positions, resulting in large initial errors. During straight-line flight, the formation error is less than 0.1 m, and during coordinated turns, the formation error is less than 1.9 m. At 40 seconds into formation flight, the ground station sends a formation dispersion command to execute a reconnaissance mission; at 90 seconds, the formation regrouped and flew to the next target. Upon receiving the formation adjustment command, the longitudinal and lateral formation errors of each UAV undergo sudden changes but converge to near zero within 6 seconds. This indicates that the controller rapidly compensates for disturbance errors when subjected to external disturbances, achieving stable formation maintenance control.

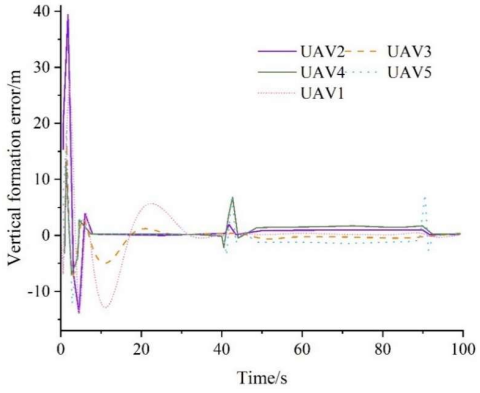

Figure 10: Error of vertical formation of each UAV

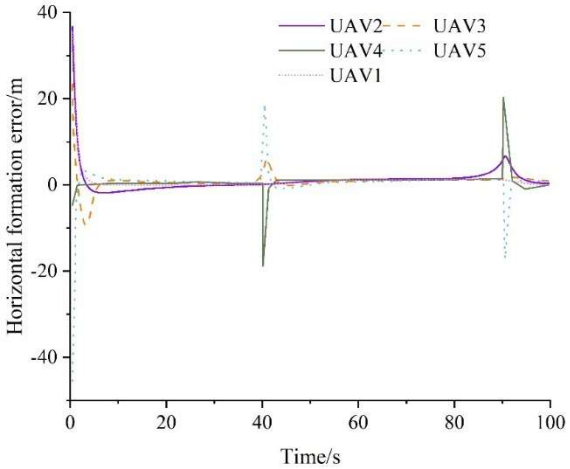

Figure 11: Error in lateral formation of each UAV

Since the positions of each UAV in the formation are relatively fixed in space, they can be regarded as a virtual rigid body composed of multiple nodes. When the rigid body turns, nodes on the same curvature radius have the same heading, while

nodes behind that node have a certain phase lag in their heading angles. Therefore, the farther a UAV is from the virtual leader in the longitudinal direction, the larger its heading angle error will be, and vice versa. The heading angle tracking errors of each UAV relative to the virtual leader are shown in Figure 12. Due to the formation definition, UAV4 and UAV5 are located 30m longitudinally from the virtual leader, resulting in a heading angle error of 0.35rad during turning maneuvers. In contrast, the UAV closest to the virtual leader longitudinally (only 10m away) has an error of just 0.13rad.

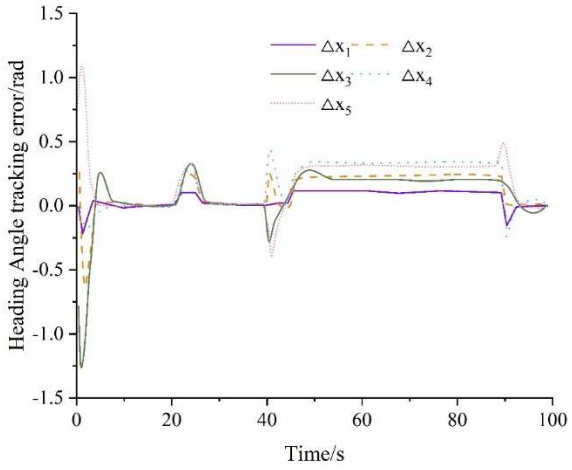

Figure 12: Tracking error of each UAV to the virtual long aircraft heading Angle

The formation is defined in the wingman's heading coordinate system. When the heading angle tracking error is not zero, it inevitably leads to formation errors. As analyzed above, during coordinated turns, the heading angle of the UAV, which maintains a certain longitudinal distance from the virtual lead aircraft, lags behind that of the virtual lead aircraft, resulting in a non-zero heading angle error, which ultimately causes formation errors. The maximum formation error after coordinated turning flight stabilization is shown in Table 4, and it can be seen that its value is roughly proportional to the desired longitudinal distance and heading angle error of the formation.

Table 4: Coordinate heading error and maximum formation error during turn

UAV	UAV1	UAV2	UAV3	UAV4	UAV5
Fore-and-aft distance /m	15	25	25	35	35
Heading error/rad	0.14	0.24	0.25	0.36	0.36
Maximum formation error/m	0.09	1.33	-1.36	1.66	-1.82

The simulation results above indicate that the proposed distributed cooperative formation control algorithm enables UAVs to maintain formation effectively. Each UAV does not need to assume knowledge of the virtual lead aircraft's state but instead estimates it in real-time through the communication topology; upon receiving formation adjustment commands, it can respond swiftly, achieving formation dispersion and aggregation; when the virtual lead aircraft performs a maneuvering turn, it achieves stable following, with inner-side UAVs reducing their flight speed and outer-side UAVs increasing their flight speed during the coordinated turn, thereby accomplishing high-precision formation maintenance.

IV. C. 2) Simulation and verification of collision avoidance control strategies

Collision avoidance control has always been a key focus and challenge in drone formation research. This simulation experiment takes a Leader-Follower formation system consisting of one lead drone and two wing drones as its research subject, employing a bidirectional communication information exchange topology to simulate and validate the effectiveness of collision avoidance control methods for drone formations.

In the drone formation simulation system, the initial distance between the lead drone UAV1 and the wing drones UAV2 and UAV3 is set to 100m. The initial spacing between wing drones 1 and 2 is set to 140m. The initial formation is an isosceles right triangle, with the threat zone radius set to 80m for all drones. When adjacent drones enter the threat zone, the collision avoidance control strategy is automatically activated. During the flight of the drone formation in a triangular formation, at a certain moment, the target positions of the two wingmen UAV2 and UAV3 are set to the same point through formation transformation. The initial simulation parameters are shown in Table 5, and the comparison of the distances between the two wingmen with and without collision avoidance control methods is shown in Figure 13.

As shown by the orange curve, after the simulation begins, the drone formation flies according to the initial triangular formation. At 115 seconds, a control command is sent to change the formation, setting the target positions of the two wingman UAVs (UAV2 and UAV3) to the same point. Since the simulation system does not include an autonomous collision avoidance control method, the two wingman UAVs quickly adjust their positions, causing the distance between them to decrease sharply and eventually reach zero, resulting in a collision between the two wingman UAVs.

As shown by the purple curve, at 115 seconds after clicking to run the simulation, the target formation positions of the two wingman UAVs are set to the same point via flight control commands. The distance between the two wingman UAVs then rapidly decreases, reaching a minimum value of 63 meters at 141 seconds, preventing a collision. The distance between the two wingmen eventually stabilized at around 68 meters. This demonstrates that under the anti-collision control method, even when the target points of the two wingmen are identical, the formation system will autonomously adjust to prevent collisions between the drones, ensuring the safety of the formation.

Table 5: Simulation initial parameters

Drone number	Initial coordinate position (m)	Initial heading Angle (°)	Initial velocity (m/s)
UAV1	(0,0)	53	35
UAV2	(-75,-75)	53	35
UAV3	(75,-75)	53	35

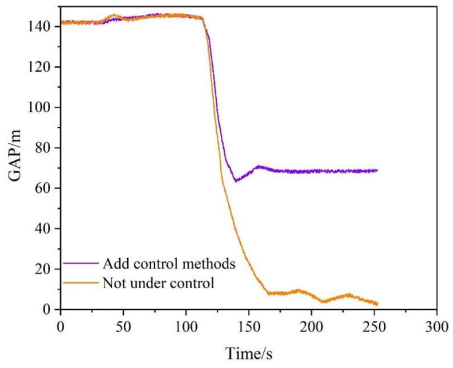

Figure 13: Comparison chart of spacing between UAV2 and UAV3 without control method

From the above simulation diagram and analysis, it can be concluded that before the collision avoidance control strategy was added, if two drones reached the same geographical location, they would not be able to avoid each other in time, resulting in a collision accident. After the collision avoidance control strategy was added to the drone formation, sufficient “repulsive force” was generated between the two approaching drones, ensuring that at any given moment, the two adjacent drones maintained a safe distance and were able to maintain formation flight.

IV. C. 3) Simulation and verification of drone formation changes

Drone formation changes refer to situations where the number of formation members remains unchanged, but the formation itself changes. After the drone formation has assembled, once the formation remains stable, the formation can be changed by adjusting the relative position variables between drones within the formation. The following simulation verification is conducted for this scenario. The initial positions, heading angles, and target position information for the formation change involving five drones are shown in Table 6, where all coordinates represent the drones' positions in the formation coordinate system. The requirement is for the drone formation to transition from a horizontal straight-line formation to a triangular formation. In both the triangular formation and the horizontal straight-line formation, the standard spacing between the lead drone and its wingman is 150 meters.

Table 6: Main parameters of formation transformation simulation

Drone number	Initial coordinate position (m)	Path angle (°)	Coordinate after formation change (m)
UAV1	(0,0)	55	(0,0)
UAV2	(-150,0)	55	(-78,-78)
UAV3	(150,0)	55	(78,-78)
UAV4	(-250,0)	55	(-149,-149)
UAV5	(250,0)	55	(149,-149)

Based on the simulation parameters in Table 6 and the formation control strategy designed in the preceding text, simulation experiments were conducted. The simulation results are shown in Figures 14 and 15.

As shown in Figures 14 and 15, from 0 to 100 seconds, the five UAVs flew stably in their initial horizontal line formation. At 100 seconds, the control center sent a formation change command to the lead aircraft, and both speed and heading angle underwent a process of deviating from the ideal values before eventually returning to the ideal values. To quickly reach the ideal spacing value in the x-direction, the maximum heading deviation was 4.8°, and the x-direction spacing adjustment was completed around 242 seconds. During the transition from the horizontal straight-line formation to the triangular formation, the speed deviated from the ideal value by a maximum of 1.6 m/s. Around 353 seconds, the y-direction spacing was adjusted to the ideal value, and the speeds of all UAVs stabilized at 34 m/s, and the heading angle stabilized at 50°, thereby achieving formation changes during formation flight.

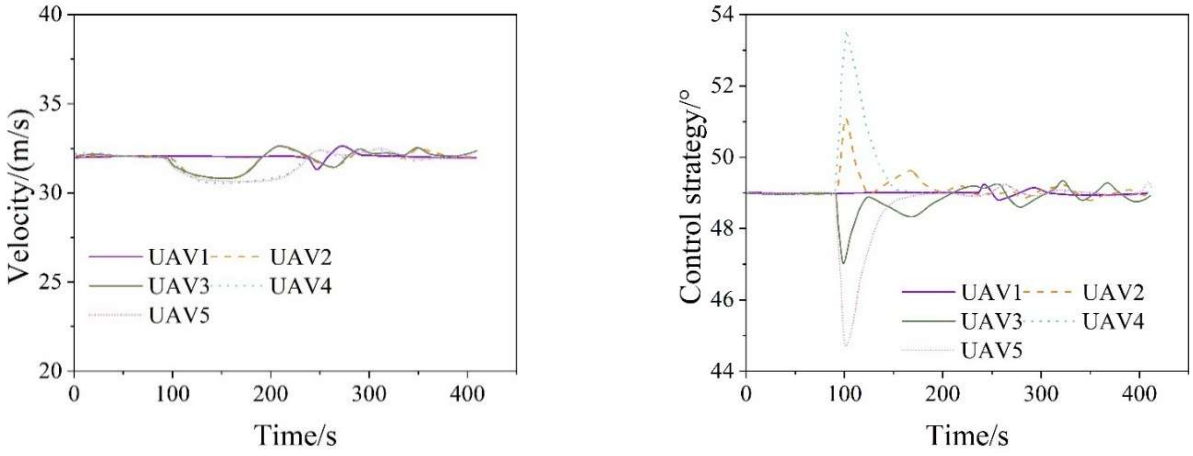

(a) Flight speed changes (b) Heading Angle variation

Figure 14: Formation change duration and wingman attitude curve

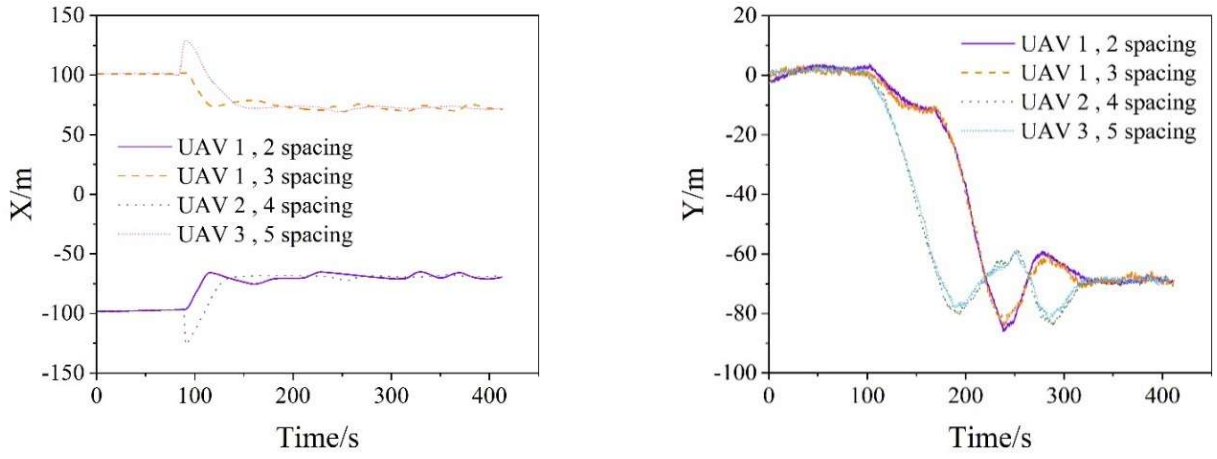

(a) X direction spacing variation (b) Y direction spacing variation

Figure 15: Change the duration of formation and the spacing between wingmen

V. Conclusion

Based on a simplified drone dynamics model, this study proposes a drone motion model based on the relative positions of drones in a three-dimensional space. It also analyzes the cooperative mechanisms of multiple drones and designs a consistency-based cooperative formation controller. The Hungarian algorithm is employed to minimize the distance cost during formation changes in a drone swarm. Simulation experiments are designed, and a triangular formation is adopted during formation maintenance simulations. Experimental results show that each UAV can accurately estimate the motion state of the virtual lead UAV in real time through the cooperative formation controller, serving as guidance for formation flight. The

control strategy enables multiple UAVs to assemble into a fixed formation, maintain the formation in various environments, avoid collisions between adjacent UAVs during formation flight, and transition to a specified formation when receiving formation transformation commands.

Funding

This work was supported by the Linxia Power Supply Company, State Grid Corporation of China (No.: B727142400XL).

References

[1] Li, B., Fei, Z., & Zhang, Y. (2018). UAV communications for 5G and beyond: Recent advances and future trends. IEEE Internet of Things Journal, 6(2), 2241-2263.
[2] Ullah, Z., Al-Turjman, F., & Mostarda, L. (2020). Cognition in UAV-aided 5G and beyond communications: A survey. IEEE Transactions on Cognitive Communications and Networking, 6(3), 872-891.
[3] Weiss, M. (2018). How to become a first mover? Mechanisms of military innovation and the development of drones. European Journal of International Security, 3(2), 187-210.
[4] Paucar, C., Morales, L., Pinto, K., Sánchez, M., Rodríguez, R., Gutierrez, M., & Palacios, L. (2018). Use of drones for surveillance and reconnaissance of military areas. In Developments and Advances in Defense and Security: Proceedings of the Multidisciplinary International Conference of Research Applied to Defense and Security (MICRADS 2018) (pp. 119-132). Springer International Publishing.
[5] Rejeb, A., Abdollahi, A., Rejeb, K., & Treiblmaier, H. (2022). Drones in agriculture: A review and bibliometric analysis. Computers and electronics in agriculture, 198, 107017.
[6] Ren, Q., Zhang, R., Cai, W., Sun, X., & Cao, L. (2020, February). Application and development of new drones in agriculture. In IOP conference series: earth and environmental science (Vol. 440, No. 5, p. 052041). IOP Publishing.
[7] Zhang, J., Yan, J., & Zhang, P. (2020). Multi-UAV formation control based on a novel back-stepping approach. IEEE Transactions on Vehicular Technology, 69(3), 2437-2448.
[8] Guo, K., Li, X., & Xie, L. (2020). Simultaneous cooperative relative localization and distributed formation control for multiple UAVs. Science China. Information Sciences, 63(1), 119201.
[9] Zhang, X., Zhang, F., & Huang, P. (2023). Formation planning for tethered multirotor UAV cooperative transportation with unknown payload and cable length. IEEE Transactions on Automation Science and Engineering.
[10] Zhang, B., Lv, M., Cui, S., Bu, X., & Park, J. H. (2024). Learning-based optimal cooperative formation tracking control for multiple UAVs: A feedforward-feedback design framework. IEEE Transactions on Automation Science and Engineering.
[11] Wadood, A., Yousaf, A. F., & Alatwi, A. M. (2024). An Enhanced Multiple Unmanned Aerial Vehicle Swarm Formation Control Using a Novel Fractional Swarming Strategy Approach. Fractal and Fractional, 8(6), 334.
[12] Stolfi, D. H., & Danoy, G. (2022). An evolutionary algorithm to optimise a distributed UAV swarm formation system. Applied Sciences, 12(20), 10218.
[13] Bu, Y., Yan, Y., & Yang, Y. (2024). Advancement challenges in UAV swarm formation control: A comprehensive review. Drones, 8(7), 320.
[14] Chen, Q., Jin, Y., Wang, T., Wang, Y., Yan, T., & Long, Y. (2022). UAV formation control under communication constraints based on distributed model predictive control. IEEE Access, 10, 126494-126507.
[15] Zhang, J., Yan, J., Zhang, P., & Kong, X. (2018). Collision avoidance in fixed-wing UAV formation flight based on a consensus control algorithm. IEEE access, 6, 43672-43682.
[16] Yang, Y., Xiong, X., & Yan, Y. (2023). UAV formation trajectory planning algorithms: A review. Drones, 7(1), 62.
[17] Park, S., Kim, K., Kim, H., & Kim, H. (2018). Formation control algorithm of multi-UAV-based network infrastructure. Applied Sciences, 8(10), 1740.
[18] Lee, D., Kim, S., & Suk, J. (2018). Formation flight of unmanned aerial vehicles using track guidance. Aerospace science and technology, 76, 412-420.
[19] Kahagh, A. M., Pazooki, F., Haghighi, S. E., & Asadi, D. (2022). Real-time formation control and obstacle avoidance algorithm for fixed-wing UAVs. The Aeronautical Journal, 126(1306), 2111-2133.
[20] Do, H. T., Hua, H. T., Nguyen, M. T., Nguyen, C. V., Nguyen, H. T., Nguyen, H. T., & Nguyen, N. T. (2021). Formation Control Algorithms for Multiple-UAVs: A Comprehensive Survey. EAI Endorsed Trans. Ind. Networks Intell. Syst., 8(27), e3.
[21] Wang, R., Lungu, M., Zhou, Z., Zhu, X., Ding, Y., & Zhao, Q. (2023). Least global position information based control of fixed-wing UAVs formation flight: Flight tests and experimental validation. Aerospace Science and Technology, 140, 108473.
[22] Muslimov, T. Z., & Munasypov, R. A. (2018, September). UAV formation flight using non-uniform vector field and fuzzy self-tuning PD-control. In 2018 International Russian Automation Conference (RusAutoCon) (pp. 1-6). IEEE.
[23] Lwowski, J., Majumdar, A., Benavidez, P., Prevost, J. J., & Jamshidi, M. (2018). Bird flocking inspired formation control for unmanned aerial vehicles using stereo camera. IEEE Systems Journal, 13(3), 3580-3589.
[24] Seo, J., Kim, Y., Kim, S., & Tsourdos, A. (2017). Collision avoidance strategies for unmanned aerial vehicles in formation flight. IEEE Transactions on aerospace and electronic systems, 53(6), 2718-2734.
[25] Bian, L., Sun, W., & Sun, T. (2019). Trajectory following and improved differential evolution solution for rapid forming of UAV formation. IEEE Access, 7, 169599-169613.
[26] Gao, S., & Zeng, C. (2023, August). A dense formation control method for UAVs based on improved ant colony algorithm. In Sixth International Conference on Advanced Electronic Materials, Computers, and Software Engineering (AEMCSE 2023) (Vol. 12787, pp. 357-362). SPIE.
[27] Yang, Z., Yang, F., Mao, T., Xiao, Z., Han, Z., & Xia, X. (2023). Reconfiguration for UAV formation: A novel method based on modified artificial bee colony algorithm. Drones, 7(10), 595.
[28] Chen, J., Chen, Y., Nie, R., Liu, L., Liu, J., & Qin, Y. (2024). Application of improved grey wolf model in collaborative trajectory optimization of unmanned aerial vehicle swarm. Scientific Reports, 14(1), 17321.
[29] Gao, C., Ma, J., Li, T., & Shen, Y. (2023). Hybrid swarm intelligent algorithm for multi-UAV formation reconfiguration. Complex & Intelligent Systems, 9(2), 1929-1962.

[30] Hoang, V. T., Phung, M. D., Dinh, T. H., & Ha, Q. P. (2018, October). Angle-encoded swarm optimization for uav formation path planning. In 2018 IEEE/RSJ International Conference on Intelligent Robots and Systems (IROS) (pp. 5239-5244). IEEE.
[31] Zhang, J., Yan, J., & Zhang, P. (2018). Fixed-wing UAV formation control design with collision avoidance based on an improved artificial potential field. IEEE Access, 6, 78342-78351.
[32] Wang, N., Dai, J., & Ying, J. (2021). UAV formation obstacle avoidance control algorithm based on improved artificial potential field and consensus. International Journal of Aeronautical and Space Sciences, 22(6), 1413-1427.
[33] Wu, E., Sun, Y., Huang, J., Zhang, C., & Li, Z. (2020). Multi UAV cluster control method based on virtual core in improved artificial potential field. IEEE Access, 8, 131647-131661.
[34] Guerrero-Castellanos, J. F., Vega-Alonzo, A., Durand, S., Marchand, N., Gonzalez-Diaz, V. R., Castañeda-Camacho, J., & Guerrero-Sánchez, W. F. (2019). Leader-following consensus and formation control of VTOL-UAVs with event-triggered communications. Sensors, 19(24), 5498.
[35] DURDU, A., & KAYABAŞI, A. (2024). Consensus-based virtual leader tracking algorithm for flight formation control of swarm UAVs. Turkish Journal of Electrical Engineering and Computer Sciences, 32(2), 251-267.
[36] Yang, K., Dong, W., Tong, Y., & He, L. (2022). Leader-follower formation consensus of quadrotor UAVs based on prescribed performance adaptive constrained backstepping control. International Journal of Control, Automation and Systems, 20(10), 3138-3154.
[37] Mehdi Doostinia,Davide Falabretti,Giacomo Verticale & Sadegh Bolouki. (2025). Critical Node Identification for Cyber–Physical Power Distribution Systems Based on Complex Network Theory: A Real Case Study. Energies,18(11),2937-2937.